

Elastic electron scattering by C_2F_4

C. Winstead and V. McKoy

A. A. Noyes Laboratory of Chemical Physics

California Institute of Technology, Pasadena, CA, 91125

Abstract

Recent measurements [R. Panajotovic *et al.*, J. Chem. Phys. **121**, 4559 (2004)] and calculations [C. Trevisan *et al.*, Phys. Rev. A **70**, 012704 (2004)] of the elastic electron cross section for C_2F_4 differ materially from our earlier calculations [C. Winstead and V. McKoy, J. Chem. Phys. **116**, 1380 (2002)]. Some of the differences are readily attributed to approximations made in our computations, but an overall difference in cross section magnitude above ca. 10 eV was surprising. Here we report a re-examination of the electron- C_2F_4 elastic cross section. After eliminating or minimizing various possible sources of error, we continue to predict a substantially larger cross section at higher energies.

PACS numbers: 34.80.Bm

I. INTRODUCTION

In the past few years, several studies have examined cross sections for low-energy electron collisions with tetrafluoroethene, C_2F_4 . Haaland [1] and Bart and co-workers [2] measured electron-impact ionization cross sections. As part of an effort to construct a validated electron cross section set for C_2F_4 [3], we used the Schwinger multichannel (SMC) method [4, 5] to calculate cross sections for elastic scattering and electronic excitation [6]. Szmytkowski and co-workers [7] measured the total electron-scattering cross section. More recently, Panajotovic and co-workers reported measurements of the elastic differential cross section (DCS) [8, 9], and Trevisan and co-workers reported corresponding calculations using the Kohn variational method and incorporating an extensive treatment of polarization [10].

The two recent determinations of the elastic cross section disagree with our earlier results in several ways, some expected and some unexpected. Specifically, because our treatment of polarization was limited and because we worked in the fixed-nuclei approximation, we expected our results to disagree with measurements or more elaborate calculations at the lowest energies and in the presence of strong resonances. On the other hand, we expected our results to be quite accurate at energies above about 10 eV, where polarization effects are less important, yet there are in fact marked differences in magnitude between our results and the measurements even at higher energies, leading Panajotovic and co-workers to state that the SMC calculation “greatly overestimates the cross section at low and high energies” [9]. Meanwhile, at higher energies the results from the recent calculation [10] differ from ours both in magnitude and in the shape of the DCS but agree fairly well in magnitude with the measured values.

Although elastic cross sections are intrinsically important both as fundamental dynamical information and for their relevance to electron transport, they are also highly important in the indirect determination of cross sections that are smaller and less easy to measure or calculate. Thus, revising the estimate of the elastic cross section calls into question [11] the entire cross-section set for C_2F_4 [3], and in the higher-energy region will strongly affect the derived value of the cross section for neutral dissociation, which is an important quantity in plasma modeling and has not yet been measured. For future applications of the SMC method, too, it is important to understand whether previously-unsuspected sources of error might exist. Accordingly, we have undertaken a detailed re-examination of elastic electron

collisions with C_2F_4 . The results of that study, reported below, indicate that our previously reported [3, 6] values for the integral and differential cross sections above are basically converged in the energy range (roughly 10 to 50 eV) where we expected them to be most reliable. Although part of the disagreement with experiment can be explained by the single-channel approximation used in the calculations, we have not identified any sources of error in the calculation sufficient to account for the increasing discrepancy in magnitude between the calculated and measured [9] elastic cross sections at higher energies. The results from the Kohn calculation also are somewhat smaller than ours at 15 and 20 eV.

II. COMPUTATIONAL DETAILS

The SMC method [4, 5] and its implementation have been described previously [12, 13]; here we give only those details specific to the present study.

The calculations reported here employed the aug-cc-PVTZ basis set of Dunning and co-workers [14], omitting the f Gaussians but including all polarization functions. We excluded the $x^2 + y^2 + z^2$ linear combination of the d Gaussians. The resulting basis set is similar in size to, but completely independent of, the basis set used in the earlier SMC calculation [6]. As before, we worked in the fixed-nuclei approximation at the experimental geometry [15].

As a Schwinger-type method, the SMC method requires matrix elements involving the free-particle Green's function. We evaluate these using the spectral representation of the Green's function and a three-dimensional numerical quadrature in which the integration variable is a wave vector, \vec{k} . That quadrature is performed as the product of a radial quadrature (in the magnitude, k) and an angular quadrature (in the solid angle, \hat{k}); for the latter, we employ the efficient spherical quadratures of Lebedev [16]. Although our previous work [6] employed what we believed to be a sufficient quadrature grid, as part of the present study we modified our code to permit larger grids and then examined the convergence of the quadrature by carrying out a series of calculations at the static-exchange level (that is, omitting polarization). Changes at the higher energies were minor. At lower energies, resonance positions shifted somewhat with better quadratures, but the major effects were seen in 2A_g symmetry at the lowest energies, where the cross section magnitude proved quite sensitive to far-off-shell contributions to the Green's function. We continued improving the radial quadrature until adding substantially more points resulted in changes to the static-

exchange integral cross section of less than 1%. We then improved the angular quadrature until, again, addition of substantially more points resulted in changes of less than 1%. The quadrature that gave results within 1% of the best result was then used in the calculations incorporating polarization effects. For the on-shell portion of the calculation, we mostly used Lebedev quadrature of order $\ell = 23$, and we retained partial waves up to $\ell = 16$ when expanding linear-momentum scattering amplitudes obtained on that quadrature grid to perform the angle averages needed to extract laboratory-frame DCS. In static-exchange calculations above 30 eV, however, we used larger quadratures (up to $\ell = 47$) and retained more partial waves where necessary to obtain convergence.

Additional differences between the previous calculation [6] and the present calculation are summarized below:

$^2B_{2g}$ Symmetry: In the earlier work, we represented polarization through terms $\mathcal{A}[(h \rightarrow p)\tilde{b}_{2g}]$, where \mathcal{A} is an antisymmetrizer, $(h \rightarrow p)$ is a 1A_g state formed from the Hartree-Fock ground state of C_2F_4 by single excitation from valence orbital h to virtual orbital p , and \tilde{b}_{2g} is a compact, resonance-like b_{2g} (π^*) orbital formed from the b_{2g} virtual orbitals. In the present work, we also include terms $\mathcal{A}[(2b_{3u} \rightarrow nb_{3u})\tilde{b}_{2g}]$ formed from *triplet* excitations out of the $2b_{3u}$ (π) orbital. Including terms formed from both the triplet and singlet ($2b_{3u} \rightarrow nb_{3u}$) excitations is equivalent, after antisymmetrization, to including both $(2b_{3u} \rightarrow \tilde{b}_{2g})^3B_{1u}$ and $(2b_{3u} \rightarrow \tilde{b}_{2g})^1B_{1u}$ as closed channels.

2A_g Symmetry: In the previous study, we treated this symmetry at the static-exchange level, applying an *ad hoc* correction at low energy. In the present work, polarization is treated in a manner similar to that employed by Trevisan and co-workers [10], including both dipole-allowed excitations of the target into orbitals designed to capture the long-range polarization response and dipole-forbidden excitations intended to capture resonance-relaxation effects. To represent long-range polarization, we included the 81 excitations out of the 12 outermost orbitals that had a dipole matrix element larger than 0.1 atomic units. The dipole-forbidden excitations included both the triplet analogues of the dipole-allowed singlet excitations and a further set of symmetry-preserving singlet excitations out of all 18 inner- and outer-valence orbitals in the presence of the first 3 a_g polarized orbitals. The total space consisted of 5002 2A_g configuration state functions (CSF's).

$^2B_{3u}$ and $^2B_{3g}$ Symmetries: These symmetries were treated in the static-exchange approximation previously. We now include polarization effects, using symmetry-preserving sin-

glet excitations of the target in the presence of compact \tilde{b}_{3u} and \tilde{b}_{3g} orbitals. For ${}^2B_{3u}$ symmetry, we also examined the effect of treating polarization along the lines of the “polarized-SCF” treatment employed by Trevisan and co-workers for both ${}^2B_{3u}$ and ${}^2B_{3g}$ symmetries—that is, employing dipole-allowed excitations into a set of orbitals optimized to capture the long-range polarization response. We used the same set of 81 dipole-allowed singlet excitations from the outer 12 valence orbitals that we used for 2A_g symmetry to build a set of ${}^2B_{3u}$ $(N + 1)$ -particle configurations, which gave a total of 1539 ${}^2B_{3u}$ CSF’s.

III. RESULTS AND DISCUSSION

Panajotovic and co-workers [9] directly measured differential cross sections, placed them on an absolute scale using the relative-flow technique [17, 18], and obtained integral and momentum-transfer cross sections by integration after extrapolating to 0 and 180°. Likewise, the direct result of calculations is angle-dependent information. The Kohn calculations for C_2F_4 produced partial-wave scattering amplitudes up to $(\ell, m) = 6$, while the SMC calculations produced linear-momentum scattering amplitudes, and in each case the amplitudes were appropriately angle-averaged to produce differential cross sections, from which integral and momentum-transfer cross sections were then obtained by integration. We can best understand the agreement and disagreement among the various results, therefore, by examining the differential rather than the integral values.

Fig. 1 shows measured and computed differential cross sections at 10, 15, 20, and 30 eV. (The SMC results at 30 eV are obtained at the static-exchange level.) At 10–30 eV, we expect our calculations to be most reliable: polarization and resonance effects are less critical than at lower energies, and incorporating a good representation of high partial waves is less important than at higher energies. Nonetheless, it is clear from Fig. 1 that our results are not in close agreement with the experimental data; indeed, except for a few angles at 10 eV, the SMC results are everywhere larger than the measurements. Similar results were obtained (at the static-exchange level) in our previous study [6], although the present results agree somewhat better in *shape* with the experimental data than do our previous DCS. The DCS calculated by the Kohn method [10], on the other hand, are closer in magnitude to the experimental results than ours but less similar in shape: the minima occur at somewhat different angles, and both the minima and the backscattering peaks are less pronounced

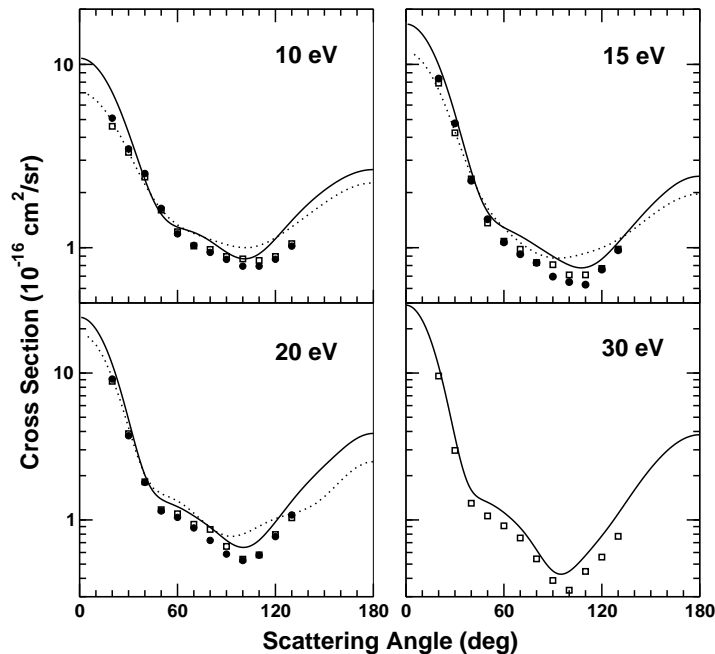


FIG. 1: Differential cross sections for elastic scattering of electrons by C_2F_4 at energies from 10 to 30 eV. Shown are the results of the present calculation (solid line), the calculation of Ref. [10] (dotted line), and the measured values of Ref. [9] (circles and squares).

than in the measurements. The largest absolute differences between the calculations occur, of course, at forward angles where the DCS is largest.

In Fig. 2, we again compare our DCS at 10, 15, 20, and 30 eV to experiment, but this time we have scaled the experimental DCS uniformly by a factor of 1.2. As may be seen, the resulting agreement is fair at 10 eV and excellent at 15, 20, and 30 eV; indeed, the agreement at the latter three energies seems to us far too good to be coincidental. Having taken care, as described in the preceding section, to minimize errors in the calculation, we conclude that either some heretofore unconsidered source of error affects the calculation, or the experimental values as reported [9] and as shown in Fig. 1 are too small. We will discuss below one source of calculational error that might explain some, but not all, of the discrepancy. We also note that the same analysis, which required some assumptions about the C_2F_4 gas dynamics, was used to place both sets of measurements on an absolute scale [9], though it would be surprising if those assumptions led to errors in the 20% range [19].

It is natural to ask whether the same scaling factor leads to good agreement at other energies. We turn first to the two higher energies where measurements were made, 60 and

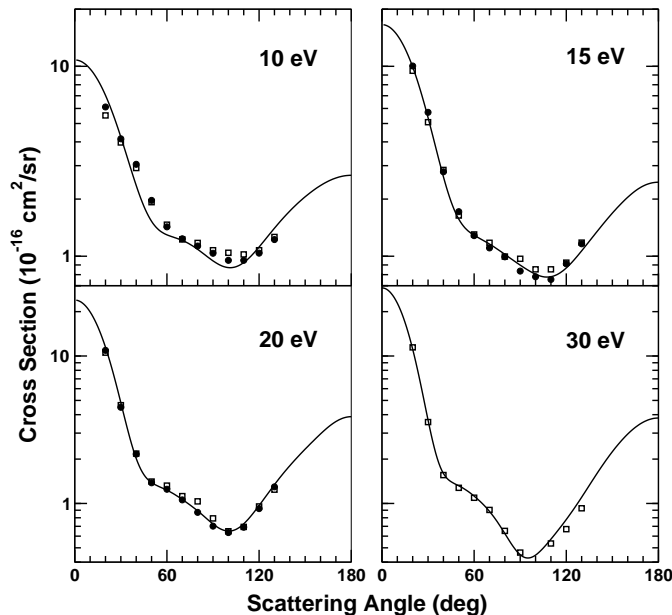


FIG. 2: Differential cross sections for elastic scattering of electrons by C_2F_4 from 10 to 30 eV. The solid line is the present calculation; the circles and squares are measured values of Ref. [9] multiplied by a factor of 1.2.

100 eV. Fig. 3 compares our static-exchange DCS to those measurements, both unscaled and with scaling factors applied. Clearly, scaling by 1.2 would not bring the experimental and SMC DCS into agreement, but fair agreement is achieved with larger factors, roughly 1.8 at 60 eV and 2.2 at 100 eV, although there are differences in the shape of the DCS that no simple scale factor can account for. We believe these differences in shape primarily reflect basis-set limitations in our calculation. It becomes increasingly difficult for a given basis set to reproduce well the nodal structure of the wavefunction at higher energies, where more partial waves contribute and the de Broglie wavelength of the projectile is shorter. In support of this interpretation, the dotted lines in Fig. 3 show results from a test calculation in which we augmented the basis set with additional s and p Gaussians on centers laid out parallel to the C-C axis but above and below the molecular plane. Though the changes are minor, they are in the right direction, bringing the shape of the calculated DCS closer to that of the measured DCS. In particular, there is stronger forward peaking and the behavior near the minimum is improved, especially at 100 eV.

The differences in overall magnitude at 60 and 100 eV are more difficult to account for than the differences in shape. The basis-set limitations just discussed will of course have

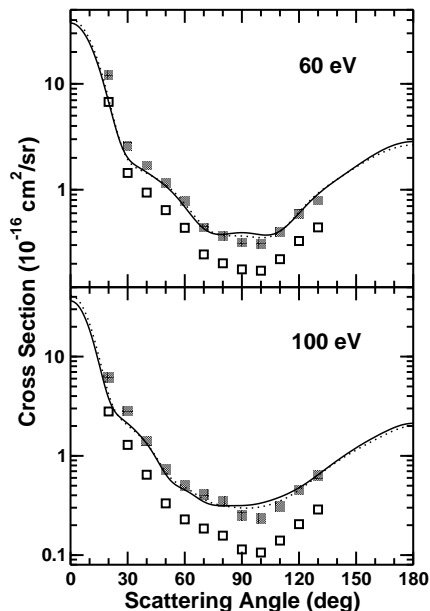


FIG. 3: Differential cross sections for elastic electron scattering by C_2F_4 at 60 and 100 eV. Shown are results of the present calculation using the same basis set as in Fig. 1 (solid line) and the extended basis set described in the text (dotted line), as well as the measurements of Ref. [9] (open squares). The filled squares are obtained by multiplying the measured values by 1.8 at 60 eV and by 2.2 at 100 eV.

some effect on the magnitude as well as the angular variation of the cross section, but they appear highly unlikely to lead to gross errors in the magnitude. The cross-checking between independent measurements that was possible at energies up to 20 eV was not possible at 30, 60, and 100 eV, where only one set of data was obtained [19], so greater uncertainty at the latter energies is perhaps to be expected; nevertheless, considered alongside the results at 10 to 30 eV, the results at 60 and 100 eV appear to indicate that the analysis used to place the measured DCS on an absolute scale underestimates the actual DCS by an amount that *increases as a function of energy* and becomes quite large (a factor of 2 or more) by 100 eV.

Such a conclusion might well be thought tenuous if based solely on comparison with our calculations, but an independent argument based entirely on experimental data also suggests that the results of Panajotovic and co-workers are too small at higher energies. Fig. 4 shows three types of measured cross section for C_2F_4 : the integral elastic cross sections obtained by Panajotovic and co-workers from their elastic DCS; the cross section for electron-impact ionization, summed over all product ions, as measured by Bart and co-workers [2] (which

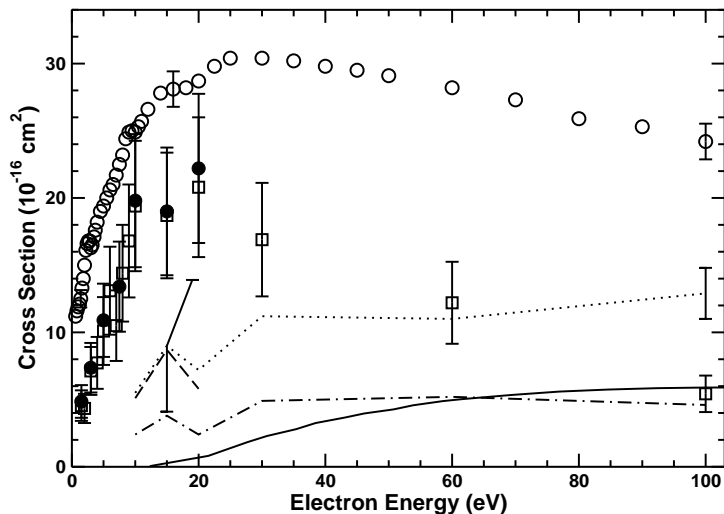


FIG. 4: Measured and derived electron- C_2F_4 cross sections. Open circles are the total collision cross section from Ref. [7], filled circles and open squares are the integral elastic cross sections of Ref. [9], and the solid line is the ionization cross section of Ref. [2]. Derived cross sections for all inelastic processes yielding neutral products, based on the integral elastic cross sections of Ref. [9], are shown by the dotted and long-dashed lines. The dot-dash line is the derived neutral-inelastic cross section based on the present calculation of the integral elastic cross section. See text for discussion.

agrees well with the ionization cross section of Haaland [1]); and the total cross section for electron scattering measured by Szmytkowski and co-workers [7]. Subtracting the elastic and ionization cross sections from the TCS yields the cross section for all inelastic processes that produce neutral products (principally electronic and vibrational excitation, including dissociative excitation leading to neutral fragments). Fig. 4 shows such neutral-excitation cross sections as derived from the elastic results of Panajotovic and co-workers and as derived from our calculations (using static-exchange results above 20 eV). The error bars shown for the former at 15 and 100 eV are root-mean-square combinations of the reported uncertainties in the total [7], elastic [9], and ionization [2] cross sections. At low energies, the difference between the two neutral-excitation cross sections can be accounted for by the uncertainty in the underlying data. At higher energies, however, the difference is significant. The integral elastic cross section reported by Panajotovic and co-workers implies a very large neutral-inelastic cross section—indeed, one that is larger at 100 eV than the measured elastic and ionization cross sections combined. The neutral-inelastic cross section implied by the SMC

elastic cross section is much smaller and, in our view, more plausible. A limitation of this argument is that it is based on a single determination of the total scattering cross section [7], but we can at least say that the experimental total and integral elastic cross sections appear to be mutually incompatible.

One source of error in our calculation (and in the Kohn calculation [10]) that we have not yet considered is the single-channel approximation. Although we include electronically excited terms in the wavefunction to represent polarization, all such excitations are treated as virtual, with elastic scattering the only open channel. In reality, of course, the energies of interest lie well above the lowest electronic thresholds, and flux can be lost into inelastic channels. We estimated the effect of the single-channel approximation by making an exploratory calculation of the elastic cross section in a three-channel approximation that included as additional open channels two of the most significant [6] electronic excitations, $(\pi \rightarrow \pi^*)^{1,3}B_{1u}$. Comparison is complicated by changes in resonance positions and shapes that are due to the three-channel calculation including only a limited representation of polarization, and by lesser numerical stability in the three-channel elastic result than in either the polarized or the static-exchange results. However, based on the general magnitude of the reductions in the cross section we observed (3% at 15 eV and 6% at 20 eV, in comparison to the polarized elastic results; 6% at 30 eV, 3% at 60 eV, and 2% at 100 eV, in comparison to the static-exchange results), we estimate that, up to 20 eV, no more than half of the disagreement with experiment is likely due to the single-channel approximation, and a much smaller proportion at the higher energies.

Turning now to lower energies, we show in Fig. 5 the DCS at selected energies below 10 eV, where it is again possible to compare our results not only to the experimental DCS [9] but also to the results obtained by the Kohn method [10]. Neither calculation agrees very well with the measured data at these energies, nor do the calculations agree well with each other. Neglect of nuclear motion in the calculations probably accounts for some of the disagreement. There are numerous shape resonances in this energy range, and the fixed-nuclei approximation tends to make those resonances too strong and too narrow while also eliminating the distinction between vibrationally elastic and vibrationally inelastic scattering. Both effects tend to overemphasize the influence of resonances on the magnitude and the angular variation of the calculated elastic cross section. However, it is also probable that the representation of polarization is not sufficient in either calculation at these energies, leading

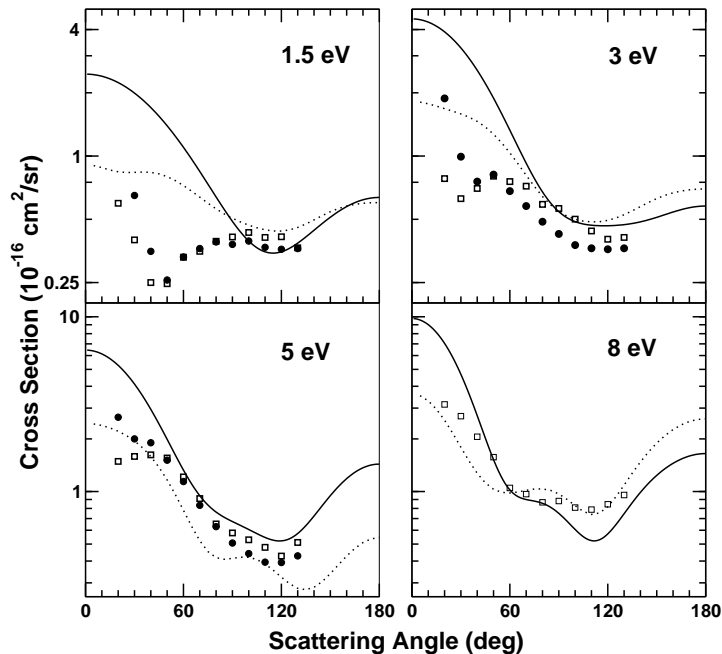


FIG. 5: As in Fig. 1, at 1.5, 3, 5, and 8 eV.

in particular to the poor agreement with experiment below 100° at 1.5 eV. Trevisan and co-workers have already noted the difficulty of fully converging the treatment of polarization in C_2F_4 [10], and our own treatment is less extensive than theirs, particularly in ${}^2B_{3g}$ and ${}^2B_{3u}$ symmetries.

Symmetry contributions to the calculated cross sections are shown in Fig. 6. Not shown are two small, nonresonant components treated at the static-exchange level: ${}^2B_{1g}$, for which both calculations gave similar results, and 2A_u , which was omitted by Trevisan and co-workers [10] and which, according to our calculations, contributes about 3% of the total at 20 eV, and less at lower energies. With the possible exception of the feature at 9.5 eV in ${}^2B_{2u}$ symmetry, jagged oscillations seen at higher energies are pseudo-resonances, which are commonly found when representing polarization via closed excitation channels beyond the lowest electronic thresholds. We see in Fig. 6 that the SMC and Kohn [10] calculations generally concur on the number, approximate widths, and profiles of the shape resonances, with some minor disagreements on their locations. The major differences in magnitude occur in 2A_g , ${}^2B_{2g}$, ${}^2B_{3g}$, and ${}^2B_{3u}$ symmetries. In 2A_g , our calculation produces a stronger maximum on the low-energy side of the broad window-and-peak resonance. In ${}^2B_{2g}$, the two calculations agree closely on the position and height of the narrow π^* resonance, but

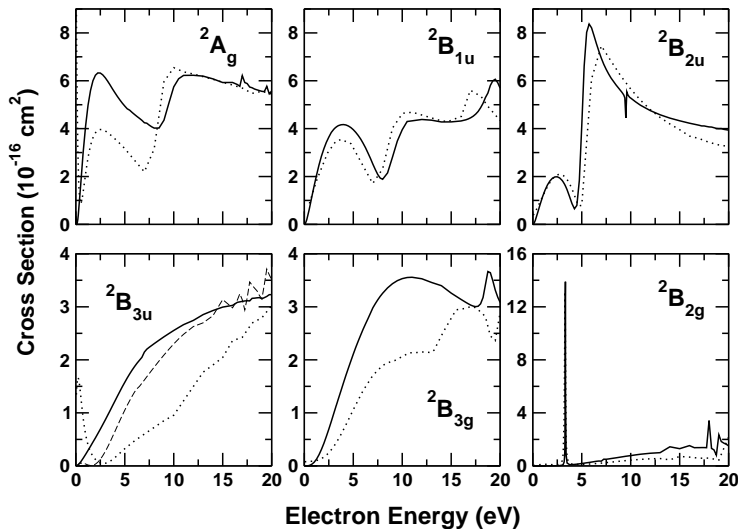


FIG. 6: Symmetry components of the integral elastic cross section for electron scattering by C_2F_4 . The six largest symmetry contributions are shown. Solid lines are the present calculations and dotted lines the calculations of Ref. [10]. The long-dashed line for ${}^2B_{3u}$ is the present result using a different treatment of polarization (see text for discussion).

above the resonance, the Kohn results are much smaller than the SMC results over a wide energy range. In ${}^2B_{3g}$ and ${}^2B_{3u}$ symmetries, the Kohn calculations indicate a significant suppression of the cross section (compared to static-exchange values [10]) below ~ 15 eV when using a “polarized SCF” treatment of polarization. Our calculation, using a treatment similar in spirit to their “relaxed SCF” approach, produces much smaller changes from the static-exchange results. We also tested a treatment equivalent to polarized SCF in ${}^2B_{3u}$ symmetry (long-dashed line in Fig. 6); although there was some reduction of the low-energy cross section, we did not find the dramatic effect seen by Trevisan and co-workers. This may well be because our treatment of polarization was less extensive, but the unusual form of the polarized Kohn results for ${}^2B_{3u}$ and ${}^2B_{3g}$ and the fact that differences were already seen at the static-exchange level make it difficult to draw firm conclusions.

With the background developed by considering the preceding results, we now examine the integral and momentum-transfer elastic cross sections, shown respectively in Figs. 7 and 8. As seen in Fig. 7, the more extensive treatment of polarization in the present work leads to a significant decrease in the magnitude of the integral cross section between roughly 3 and 10 eV compared to our earlier results [6], but the decrease above 10 eV is much smaller. The Kohn integral cross section is close to the experimental values in magnitude from 5 to 20 eV;

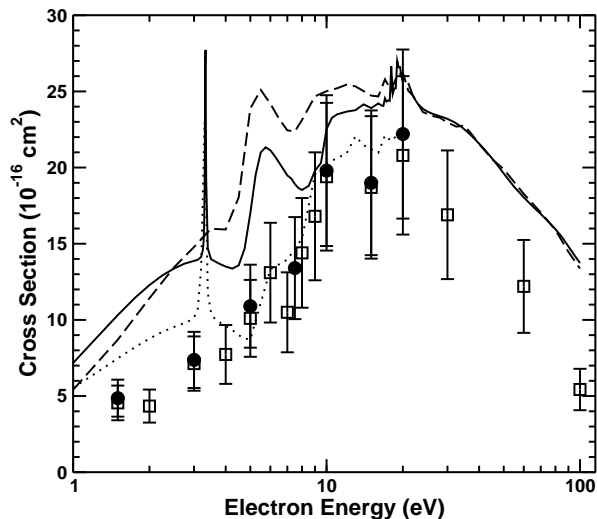


FIG. 7: Integral cross section for elastic scattering of electrons by C_2F_4 . Solid line is the present calculation (using the static-exchange approximation above 20 eV), dotted line the calculation of Ref. [10], long-dashed line our previous calculated result, Ref. [6], and squares and circles the experimental values of Ref. [9].

however, as was shown in Figs. 1 and 5, the DCS from which it is obtained differ considerably in their angular dependence from the corresponding measured DCS. As we have discussed, the differences below 10 eV probably originate in the fixed-nuclei approximation and an incomplete representation of polarization. Above 10 eV, the omission of 2A_u in the Kohn calculation and the differences in ${}^2B_{3g}$ and ${}^2B_{3u}$ symmetry seen in Fig. 6 explain part of the difference between the calculations. Given the size of the target molecule, it is also natural to suspect that the restriction of the Kohn scattering-amplitude calculation to angular momenta less than or equal to $(\ell, m) = 6$ might be involved. However, test calculations extending the Kohn static-exchange results in several symmetries to higher partial waves did not produce significant changes in the integral cross section [20]. Because the DCS is more sensitive to partial-wave convergence, underrepresentation of high-partial-wave contributions in the Kohn results may nonetheless account for much of the disagreement in the shape of the DCS (Fig. 1). Higher partial waves can be important to building up peaks at forward and backward angles, as well as to building in minima at intermediate angles, even when they contribute relatively little to the angle-integrated cross section.

Agreement between the SMC and Kohn calculations is on the whole somewhat better for the momentum-transfer cross section, Fig. 8, and our present results are much closer

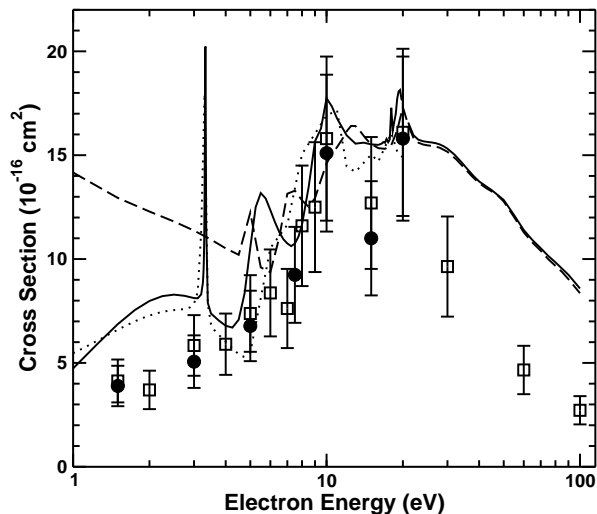


FIG. 8: As in Fig. 7, for the momentum-transfer cross section.

to experiment below 10 eV than our previous results [6]. The largest apparent errors in the SMC DCS below 10 eV are at forward angles, which are given little weight in the momentum-transfer cross section. At higher energies, the Kohn and SMC results oscillate about each other, largely reflecting disparities between the two calculations in the influence of resonances on the intermediate- and high-angle DCS. At 10 to 30 eV, the differences in magnitude between our momentum-transfer cross section and experiment are roughly comparable to those in the integral elastic cross section, except at 20 eV, where agreement is somewhat better than expected, given the discrepancies in the underlying DCS (Fig. 1).

IV. SUMMARY AND CONCLUSIONS

Improving the quality of the SMC calculation results, as expected, in significant changes to the C_2F_4 elastic cross section at low energies, and those changes bring the SMC results into closer, though still not satisfactory, agreement with recent measured [9] and Kohn [10] results. Improving the SMC calculation does not, however, affect the disagreement with the measured elastic cross sections at higher energies. Although our DCS above 10 eV appear to be converged, they differ systematically from the measurements by a factor of ~ 1.2 up to 30 eV, slightly more than the quoted experimental uncertainty, and by still larger factors at 60 and 100 eV. At 10, 15, and 20 eV, the DCS calculated by the Kohn method differ in form both from our results and from the measurements. Although going beyond the

single-channel approximation should reduce our computed cross sections, it does not appear that the reduction would be large enough to account for the disagreements seen. For these reasons, we believe the SMC results presented here are the best values currently available for the electron–C₂F₄ elastic cross section above ~ 10 eV. Certainly a revision of the C₂F₄ cross section set [3] in the low-energy region is advisable in light of the newly measured elastic and vibrational excitation cross sections [9, 11]. However, because the present values are close to our previous results [6] at higher energies, revision of the existing electron–C₂F₄ cross-section set [3] above 10 eV may not yet be in order. In particular, the cross section for inelastic processes with neutral products is probably not as large as the recent elastic measurements imply. Additional determinations of the elastic and total cross sections would be highly useful.

Acknowledgments

This work was supported by the U.S. Department of Energy, Office of Basic Energy Sciences. We acknowledge Intel Corporation for an equipment grant that provided the computer cluster where many of these calculations were run and the JPL/Caltech Supercomputer Project for additional computing resources. We thank Profs. Stephen Buckman and Ann Orel for helpful discussions, Prof. Buckman for communicating results in advance of publication, Dr. Cynthia Trevisan for providing data in electronic form, and Prof. Buckman and Dr. Trevisan for their comments on the manuscript.

-
- [1] P. D. Haaland, unpublished results, quoted in Ref. [3].
 - [2] M. Bart, P. W. Harland, J. E. Hudson, and C. Vallance, *Phys. Chem. Chem. Phys.* **3**, 800 (2001).
 - [3] K. Yoshida, S. Goto, H. Tagashira, C. Winstead, B. V. McKoy, and W. L. Morgan, *J. Appl. Phys.* **91**, 2637 (2002).
 - [4] K. Takatsuka, and V. McKoy, *Phys. Rev. A* **24**, 2473 (1981); *ibid.* **30**, 1734 (1984).
 - [5] M. A. P. Lima, L. M. Brescansin, A. J. R. da Silva, C. Winstead, and V. McKoy, *Phys. Rev. A* **41**, 327 (1990).
 - [6] C. Winstead and V. McKoy, *J. Chem. Phys.* **116**, 1380 (2002).

- [7] C. Szmytkowski, S. Kwitnewski, and E. Ptasińska-Denga, *Phys. Rev. A* **68**, 032715 (2003).
- [8] S. J. Buckman, R. Panajotovic, and M. Jelisavcic, *Phys. Scripta* **T110**, 166 (2004).
- [9] R. Panajotovic, M. Jelisavcic, R. Kajita, T. Tanaka, M. Kitajima, H. Cho, H. Tanaka, and S. J. Buckman, *J. Chem. Phys.* **121**, 4559 (2004).
- [10] C. Trevisan, A. E. Orel, and T. N. Rescigno, *Phys. Rev. A* **70**, 012704 (2004).
- [11] W. L. Morgan and S. J. Buckman, presentation at the 56th Gaseous Electronics Conference, San Francisco, October, 2003 (<http://www.kinema.com/C2F4GEC03.pdf>).
- [12] C. Winstead, and V. McKoy, *Adv. At. Mol. Opt. Phys.* **36**, 183 (1996).
- [13] C. Winstead, and V. McKoy, *Comp. Phys. Commun.* **128**, 386 (2000).
- [14] T. H. Dunning, Jr., *J. Chem. Phys.* **90**, 1007 (1989).
- [15] J. L. Carlos, R. R. Karl, and S. H. Bauer, *J. Chem. Soc. Faraday Trans. II* **70**, 177 (1974).
- [16] V. I. Lebedev and D. N. Laikov, *Dokl. Akad. Nauk* **366**, no. 6, 741 (1999) [*Dokl. Math.* **59**, no. 3, 477 (1999)], and references therein; see also <http://www.ccl.net/cca/software/SOURCES/FORTRAN/Lebedev-Laikov-Grids/index.html>.
- [17] S. K. Srivastava, A. Chutjian, and S. Trajmar, *J. Phys. Chem.* **63**, 2659 (1975).
- [18] M. Kitajima, Y. Sakamoto, R. J. Gulley, M. Hoshino, J. C. Gibson, H. Tanaka, and S. J. Buckman, *J. Phys. B* **33**, 1687 (2000).
- [19] S. J. Buckman, private communication.
- [20] C. S. Trevisan, private communication.